Magn Reson Mater Phy (2006) 19: 209–222
DOI 10.1007/s10334-006-0049-8

RESEARCH ARTICLE

Sources of variation in multi-centre brain MTR histogram studies: body-coil transmission eliminates inter-centre differences

P. S. Tofts
S. C. A. Steens
M. Cercignani
F. Admiraal-Behloul
P. A. M. Hofman
M. J. P. van Osch
W. M. Teeuwisse
D. J. Tozer
J. H. T. M. van Waesberghe
R. Yeung
G. J. Barker
M. A. van Buchem

Received: 4 April 2006
Accepted: 2 August 2006
Published online: 7 September 2006

P. S. Tofts (✉)· M. Cercignani · D. J. Tozer
G. J. Barker
Institute of Neurology, University College London, Queen Square, London WC1N 3BG, UK
Tel.: +44-20-78373611
E-mail: p.tofts@ion.ucl.ac.uk

S. C. A. Steens · F. Admiraal-Behloul
M. J. P. van Osch · W. M. Teeuwissee
M. A. van Buchem
Department of Radiology, Leiden University Medical Center, Leiden, Netherlands

P. A. M. Hofman
Department of Radiology, Maastricht University Hospital, Maastricht, Netherlands

J. H. T. M. van Waesberghe
Department of Radiology, Free University Medical Centre, Amsterdam, Netherlands

R. Yeung
GE Medical Systems, Slough, SL1 4ER, UK

P. S. Tofts
current address: Brighton and Sussex Medical School, Brighton BN1 9PX, UK

G. J. Barker
current address: King's College London, Institute of Psychiatry (Box 089), Department of Clinical Neuroscience, Centre for Neuroimaging Sciences, De Crespigny Park, London SE5 8AF, UK

Abstract *Object:* 1. Identify sources of variation affecting Magnetisation Transfer Ratio (MTR) histogram reproducibility between-centres. 2. Demonstrate complete elimination of inter-centre difference.
Materials and methods: Six principle sources of variation were summarised and analysed. These are: the imager coil used for radiofrequency (RF) transmission, imager stability, the shape and other parameters describing the Magnetisation Transfer (MT) pulse, the MT sequence used (including its parameters), the image segmentation methodology, and the histogram generation technique. Transmit field nonuniformity and B1 errors are often the largest factors. PLUMB (Peak Location Uniformity in MTR histograms of the Brain) plots are a convenient way of visualising differences. Five multi-centres studies were undertaken to investigate and minimise differences.
Results: Transmission using a body coil, with a close-fitting array of surface coils for reception, gave the best uniformity. Differences between two centres, having MR imagers from different manufacturers, were completely eliminated by using body coil excitation, making a small adjustment to the MT pulse flip angle, and carrying out segmentation at a single centre. Histograms and their peak location and height values were indistinguishable.
Conclusions: Body coil excitation is preferred for multi-centre studies. Analysis (segmentation and histogram generation) should ideally be carried out at a single site.

Keywords MRI · Brain · Magnetisation transfer · Multi-centre study

Introduction

Magnetisation transfer ratio (MTR) histograms are being used to an increasing extent to characterise subtle disease in the brain [1–3]. In a disease where the damage is diffuse and widespread (as opposed to focal), and the signal or parameter change is too small to be seen visually, then whole-brain histograms [4–6] have proved extremely effective in detecting and characterising subtle tissue degradation. The histogram is just a frequency distribution showing how many voxels there are at each value of a tissue parameter; it is usually normalised so that the total area under the curve is fixed (this reduces the effect of differing brain sizes). Extremely small changes can be detected, for example between different subgroups in multiple sclerosis (MS) [7,8] and systemic lupus erythematosus [9,10], and in serial studies of MS [11–16].

Understanding and minimising the sources of instrumental variation is vital. These limit the reproducibility between scans, whether carried out on the same MR imager, or on different imagers [17], and thus determine how small a biological change can be reliably detected [18–20]. In long-term serial studies at the same centre, an imager upgrade (software or hardware) can cause as much disruption to measurements as the differences seen between centres.

The investigations presented here took over five years to complete, and represent progress from a simple to what we believe is a rather complete understanding of factors causing variation in MTR histograms. Data were collected at four centres at 1.5 T using machines from three manufacturers. At the two main centres, several different versions of hardware and software were used. Preliminary accounts of these data have already been given [21–23].

Table 1 Sources of variation in MTR histograms

Main category	Subcategories
Imager	
1. Transmitter coil	Body coil preferred
2. Imager stability and setup	2a. Transmitter setup—accuracy
	2b. Transmitter setup—random variations
	2c. Receive stability
	2d. Subject positioning
MT pulse and sequence	
3. MT pulse	3a. Shape
	3b. Duration
	3c. Offset frequency
	3d. Amplitude or FA_{sat}
4. Pulse sequence	4a. TR′
	4b. TR
	4c. Imaging FA
	4d. Voxel size
Postprocessing	
5. Image segmentation	
6. Histogram generation	6a. Representation of image values
	6b. Despiking procedure
	6c. Representation of MTR values
	6d. Bin width (0.1 pu preferred)
	6e. Bin labelling (central is preferred)
	6f. Smoothing
	6g. Normalisation (for tissue volume, bin width)
	6h. Feature extraction

Sources of variation in MTR histograms

The following factors (summarised in Table 1) can cause the measured MTR histogram to vary. By giving a detailed description (specification) of these when reporting MT data in publications, variation is more likely to be identified and possibly reduced (although it has to be recognised that this technical information is not always available).

1. *Transmitter coil*. This determines the B_1 (transmit field) uniformity. In a perfectly spatially uniform B_1 field, a single value of MT saturation would be applied to all tissues in the brain (since the local flip angle is proportional to the local B_1 value). However a single transmit/receive (T/R) head coil is often used, where uniformity is compromised by using a closer-fitting coil to give better signal-to-noise ratio performance during reception. The resulting *transmit nonuniformity* means that the measured MTR value depends on location with respect to the coil (even for a perfectly homogeneous tissue); an example is shown in Fig. 2d. B_1 mapping has been used to map the B_1 field over the head and then make a correction to the MTR values [24,25] (since the MTR value is approximately proportional to B_1), although this procedure is not completely accurate for all tissue types. Most desirable, at least from the uniformity point of view, is transmission by a separate, large, body coil, although one should be aware that the specific absorption rate (SAR, the power deposition) may be higher than for a head coil. There will still be B_1 nonuniformity arising from the subject's head, particularly at higher static fields; however, this is not imager dependent, and hence does not contribute to any between-centre differences. Recent MR imager designs provide close-fitting high-SNR multi-array receive coils, used with body-coil transmission, and these are ideal for MTR measurement.

2. *Imager stability and setup*
   (a) *Transmitter setup – accuracy*. Generally the imager will have an auto-pre-scan (APS) procedure to adjust the transmitter output automatically to obtain the correct flip angle (FA) for the imaging radiofrequency (RF) pulses. This procedure must be disabled for subsequent images in the MTR acquisition, so that transmitter output stays constant. (This may require the permission of the scanner manufacturer, or the signing of a research agreement.) The FA may be measured in a small volume at the coil centre, or over a larger volume of tissue (e.g. the central imaging slice, or a collection of slices). In the presence of B_1 nonuniformity, the transmitter output required will differ according to the size of the volume used. The APS may not be completely accurate (i.e. there may be a systematic error, so that for example a nominal 90° pulse is consistently set as 85°); if so, even relatively small errors will produce significant consequent changes in the measured MTR value. The centre frequency and shimming, if incorrect, could also alter the local offset frequency from the intended value.
   (b) *Transmitter setup – random variations*. The setup procedure, if repeated, may produce significant random variations in the transmitter output, even if the imager hardware itself is perfectly stable; these could arise, for example, from the effects of image noise.
   (c) *Receive stability*. Any short-term receiver instability during data collection will cause variations in the measured MTR value. After the APS procedure, the nominal receiver gain should be kept fixed. (The procedure for doing this will depend on the particular imager being used, and local physicists or the manufacturer should be consulted.)
   (d) *Subject positioning*. If the transmit field is nonuniform, altering the subject's positioning within that field will almost certainly alter the B_1 distribution within the brain, and hence the MTR map.

   Note that *receive nonuniformity* (arising for example from the receiver coil) can reduce image intensity (and hence signal-to-noise ratio), but since the MTR is calculated from a ratio of images, this does not cause inaccuracy in the MTR value, although its precision may be reduced. Similarly any other factors in the receive chain (such as software gain, or the use of multi-array coils and parallel imaging) will normally divide out.

   Items (a)–(c) can be studied using phantoms (test objects), although there may be a few cases where additional sources of variation can be present in the human subject, and measurements on normal control subjects provide the ultimate test of reproducibility. Item (d) is addressed by good radiographic technique (i.e. careful (re-)positioning of the subject in the head coil, and use of pilot images to verify the head position relative to that in previous examinations). Whilst image registration cannot correct for mispositioning, it can be used to highlight and quantify any misregistration between one examination and the next.

3. *MT pulse*: the MT pulse is specified by its
   (a) Shape: this is usually Gaussian with a specified full-width at half-maximum (FWHM), or sinc (with a specified number of lobes or zero crossings). The pulse is often apodised with a Hamming, Hanning or Gaussian window to improve its profile in frequency space; a *sinc–Gauss* pulse, for example, is a sinc pulse with Gaussian apodisation. Provision of an analytical (mathematical) description removes any ambiguity, e.g. the EuroMT pulse [26] is $\exp(-0.2248\,t^2)$, with t in ms.
   (b) Duration (ms).
   (c) Offset frequency (typically 1–2kHz): since the MTR value can depend slightly on which side of free water the MT pulse is applied [27], this should be specified (note that offsets towards the lipid side of the water peak correspond to negative values).
   (d) Amplitude: sometimes the amplitude is expressed directly, as the peak value (in μT or possibly radian s^{-1}); more often the equivalent on-resonance flip angle FA_{sat} (in degrees) is given (typically 500–800°).

   In addition, two more parameters can be calculated from the pulse shape and duration. The bandwidth (BW, in Hz) defines, in the frequency domain, the approximate extent of resonant proton frequencies that will be affected; usually the FWHM is given. The effective duration of the pulse can be summarised by its FWHM in the time domain, which we call $FWHM^t$ (in ms). For a Gaussian pulse $\exp(-\alpha t^2)$, $FWHM^t = 2\sqrt{(\ln(2)/\alpha)}$, $BW = (2/\pi)\sqrt{(\ln(2)\alpha)}$, and the product $FWHM^t \cdot BW = 4\ln(2)/\pi = 0.8825$. For example the EuroMT pulse has $FWHM^t = 3.51$ ms, BW=251 Hz. The bandwidth of a sinc pulse is approximately (no. of lobes + 1)/(pulse duration); for three- and five-lobe sinc pulses this expression overestimates BW by 3–5%. These expressions assume no apodisation has been applied, although its effect is likely to be small.

   The parameters p_1 and p_2, derived from the pulse shape, give much of the relevant information about the pulse and are often useful [17]. p_1 is the area under the pulse, compared to that of a rectangular pulse of the same duration and amplitude. FA_{sat} is then related to the peak amplitude B_{sat} by:

$$FA_{sat} = \frac{180}{\pi} \gamma p_1 B_{sat} \tau_{sat}, \quad (1)$$

where τ_{sat} is the duration of the saturating pulse. Thus with $\gamma = 2.675 \times 10^8$ rad $s^{-1} T^{-1}$ (42.57 MHz T^{-1}), B_{sat} in μT, τ_{sat} in ms, this becomes $FA_{sat} = 15.33 p_1 B_{sat} \tau_{sat}$. p_2 is the area under the square of the pulse amplitude, compared to that of a rectangular pulse of the same duration and amplitude. The root-mean-square amplitude (the "*power*"), averaged over the whole sequence, is then:

$$P_{sat} = \frac{p_2}{TR' \tau_{sat}} \left(\frac{FA_{sat} \pi}{\gamma p_1 180} \right)^2. \quad (2)$$

The MTR value is (very approximately) proportional to the effective nutation rate (ENR), which is the MT pulse flip angle divided by the time between MT pulses [17]. (This relationship only gives a rough guide to the effectiveness of a pulse.) Typical values for ENR are 10–17° ms^{-1}, giving MTR values of 30–50 pu (percentage units) in white matter at 1.5 T.

4. *Pulse sequence*. The MT pulse is incorporated into an imaging sequence, which is typically a two-dimensional spin-echo [18], a two-dimensional gradient echo [26] or a three-dimensional gradient echo [4, 28, 29]. The three-dimensional gradient echo sequences are generally preferred, since good resolution and coverage can be obtained in a reasonable time [29], with minimal MT affect from the imaging pulses.

   Although the sequence should ideally have pure proton density (PD) weighting, with negligible T_1 weighting, in practice the latter is always present to some extent, depending on the TR and imaging flip angle used (in order to provide reasonable signal-to-noise ratio in a practical imaging time). T_1 weighting is important since T_1 shortens in the presence of MT saturation, and this in turn increases the measured saturated (M_s) signal and reduces the measured MTR. An upper limit to the size of the effect can be obtained by assuming the M_s signal will be fully relaxed. For white matter at 1.5 T ($T_1 = 650$ ms, [30]), and the EuroMT sequence (TR = 960 ms, FA = 20°), the unsaturated (M_o) signal loss [31] from T_1 weighting for a gradient echo is 1.75%, and this could give as much as a 1.7 pu reduction in MTR.

   The voxel size affects partial-volume effects between different tissue types, and hence the segmentation and also the consequent MTR values in voxels containing mixtures of tissue types.
   Thus the following should be specified:

   (a) TR′ the time between the start of successive MT pulses,
   (b) TR, the repetition time of the sequence,
   (c) the excitation (imaging pulse) flip angle (FA),
   (d) imaging voxel dimensions.

   In addition, if there is significant T_1 weighting, then slice geometry factors could be significant, since these can affect the amount of T_1 weighting. These factors include the slice profile [and hence the shape of the selective pulse(s)], the slice thickness and spacing, and the order in which they are collected. TE should also be specified, although provided it is short it is unlikely to make a difference to the MTR value.

   The EuroMT sequence [26] was designed to reduce between-manufacturer differences. It has been implemented on imagers from two manufacturers (General Electric, Milwaukee, USA and Siemens, Erlangen, Germany), and provides a good example of how inter-centre uniformity can be achieved. The MTR of normal white matter varies little between subjects (for a given sequence) [18] and provides a convenient way of evaluating whether sequence implementations intended to be identical are in fact so.

5. *Image segmentation*. The whole brain, and often white and grey matter, can be extracted by a (generally automatic) procedure. Automated methods are more reproducible, although their accuracy should be checked by manual review. For manual methods, a single observer at a single centre will give the least variation. Ideally segmentation is carried out on independent structural images. These may be PD, T_2 or T_1 weighted. Spatially registered three-dimensional (volume) images, collected in the same examination, are most preferable [32]. Segmentation from the MTR maps is possible; however it is likely to be less accurate, and an arbitrary decision about excluding voxels with low values of MTR, primarily in cerebro-spinal fluid (CSF), will have to be made. Variations in this procedure clearly propagate to changes in the resulting MTR histogram; for example a more aggressive removal of voxels that contain some CSF will give a histogram with a very low short left-hand tail. The procedure should be defined, and any reproducibility tests carried out should be reported. These tests could be either reanalysis of the same image data-set, using either the same or different observers, or analysis of reacquired data-sets. For given subjects, the volume of each segmented compartment (in ml) is a convenient way of comparing segmentation methods. The segmentation method crucially affects the peak height estimate, which can be a sensitive measure of clinical status [10] (see Fig. 8).

6. *Histogram generation and characterisation* [3]. The two raw-image data-sets are usually stored as integers, with sufficient resolution so that rounding errors do not contribute to image noise. These are converted to floating-point numbers. Random noise of amplitude −0.5 to +0.5 may need to be added to avoid spikes in the resulting histograms [33]. The floating-point

arithmetic is then performed to calculate the (floating-point) MTR value, usually as a percentage; using percent units (pu) avoids ambiguity. MTR maps may be stored as scaled integers.

The histogram architecture is specified by the bin width and the bin borders. For example a 30 pu bin of width 1 pu could have borders 30.0–31.0 (left-hand label), 29.5–30.5 (central label), or 29.0–30.0 (right-hand label). The precise specification of the borders affects some of the resulting histogram features, particularly peak height and location. The bins are ideally labelled by their centre, although any other label is also unambiguous provided this is clearly stated, and may sometimes be dictated by the software used. Histograms can easily be converted to central labelling by shifting their bin labels by an appropriate amount. Smaller bin widths (e.g. 0.1 pu) reduce the influence of the border definition, and the need for interpolation when making a precise characterisation of the peak, and are to be preferred, although some smoothing may then be required. Recent clinical studies using 0.1 pu bin widths have measured extremely subtle changes in MTR values (<1 pu) [16, 34], and these almost certainly would have failed if 1 pu bin widths had been used. Small bin widths also give a truer estimation of peak height; in this study a 1 pu bin width reduced the peak height by over 10% (see Fig. 8). Even with 0.1 pu bin width, there are plenty of samples in each bin (at least 200), as seen by the smooth appearance of the histograms.

Histogram normalisation is usually carried out to remove the effect of varying tissue volumes. By also taking account of bin width [3], a *fully normalised* histogram can be produced, with y-values (in units of %volume/pu, abbreviated to %vol pu^{-1}) which are almost independent of the bin width. The peak height and location are then comparable between centres, the total area under the curve is 100%vol, and the peak height and width are inversely related.

From the final histogram, features are extracted to characterise it, e.g. peak height (PH) and location (PL), percentiles, area of a tail, or mean value (although this does not need a histogram, and can be obtained directly from the segmented volume). Peaks can be characterised either by finding the greatest value in the (smoothed) histogram, or by fitting a suitable function, e.g. a parabola or Gaussian, to the histogram values within a specified range (e.g. 2 pu) of the peak. If the histogram shows signs of bimodality [35], fitting several peaks may be more appropriate than just characterising the largest one. Principle-component analysis and linear discriminant analysis have been shown to be effective in extracting relevant information from histograms [36], without the need for feature selection.

Thus the following eight factors can affect the resulting histogram, and should be controlled and specified:

(a) Representation of the image values before calculation of the MTR map
(b) Spike-removal procedure used (if any)
(c) Representation of MTR values (scaled integer, or floating point)
(d) Bin width
(e) Bin labelling
(f) Histogram smoothing used (if any)
(g) Normalisation for tissue volume and bin width (if any)
(h) Feature extraction

Small systematic changes in measured feature values across different centres or an upgrade can be dealt with by including this as a covariate in the statistical analysis, particularly if the range of MTR values or tissues is restricted [for example control white matter (WM) and normal-appearing WM], and if normal controls have been included on each side of the change.

Methods

Five studies were carried out to investigate MTR histogram variation.

Study 1: multi-centre study

MRI: six normal controls were each scanned at three primary centres A, B and C (each individual travelled to all three centres). Centres A and B had identical imagers, with body-coil excitation and a separate head receive-only coil. The imager at centre C, from a different manufacturer, had a combined transmit/receive head coil, which tapered towards the top of the head. The MT sequence at each centre, based on the EuroMT sequence [26], was identical as far as possible. The EuroMT sequence parameters are: TR = 960 ms, TE = 12 ms, imaging FA = 20°; matrix = 128×256, field of view (FOV) = 250 mm, MT pulse FA = 500°; TR′ = 40 ms (hence ENR = 12.5° ms^{-1}); offset = 1.2 kHz. Twenty-four contiguous oblique-axial 5-mm slices, parallel to the anterior commissure/posterior commisure line, were collected.

Segmentation: for all data-sets in this study, semi-automated segmentation of the whole brain was performed by one experienced operator, on a Sun workstation (Sun Microsystems Inc, Santa Clara, CA, USA) using 3DVIEWNIX software [4, 37].

Histogram matching: histogram matching was implemented to test the hypothesis that between-centre effects could be eliminated (or at least reduced) using a simple stretch of histograms from one centre to match those of another. If the difference

between centres arises only from a difference in saturating power P (i.e. we ignore B_1 nonuniformity effects), then the MTR value for a particular tissue t is $\mathrm{MTR}(t) = a(t)\,f(P)$, where $a(t)$ describes the tissue dependence of MTR (for a given power), and $f(P)$ is an unknown function (e.g. P or P^2). The MTR values measured at centres 1 and 2 are then related by:

$$\mathrm{MTR2}(t) = \left[f(P2)/f(P1)\right]\mathrm{MTR1}(t) = b\mathrm{MTR1}(t) \qquad (3)$$

and the scaling factor b is independent of tissue type. Thus a simple scaling of histograms, followed by least-squares fitting, may be enough to transform a histogram measured at centre 1 to match that when measured at centre 2. A quadratic term could perhaps be added, to represent the plateau of MTR value as power is increased, but the preliminary studies reported here indicated that this would not have been justified in this study.

Each object histogram was stretched (or compressed) to achieve minimum root-mean-square difference between the object histogram and the target histogram. The parameter b (see Eq. 3) represented the amount the object histogram MTR values were modelled as having been scaled; removing this effect made the object and target match. Histograms remained normalised to a total area (between 5 and 60 pu) of 100%; so as a histogram was stretched its peak height automatically reduced. Values below 5 pu were ignored in the normalisation procedure (to eliminate pixels that clearly were not located in the brain). Matching was carried out by minimising the root-mean-square difference between the target and the mapped object histogram, over the range 25–50 pu, as the factor b was varied. This range was chosen to include the relevant pixels in the target histogram (see Fig. 1), whilst excluding irrelevant pixels at low values of MTR.

The hypothesis that a single centre-to-centre (subject-independent) stretch would improve inter-centre differences was tested. Centres A and C were matched to B (the target). Since centres A and B gave such similar group histograms (see the Results section), individual histograms from centre A were also transformed to better match centre B, as follows: for each subject, the inter-centre transformation was found from the five remaining subjects, and used to match the subject of interest. The inter-centre differences in PH and PL for this subject were measured before and after matching. This leave-one-out (LOO) process was repeated for each of the six subjects in turn. Thus the training and evaluation processes were truly independent. All manipulations, including the least-squares minimisation, were easily carried out in a spreadsheet.

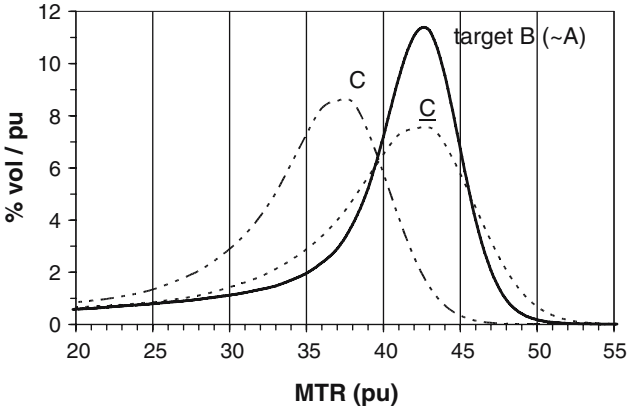

Fig. 1 Group histograms from three centres (study 1). A and B, using the same manufacturer, appear identical (hence only B is shown). An attempt was made to match mean histograms from centre C to centre B (also see Table 2). The matched histogram is labelled C. Centres A and B have body-coil excitation; centre C uses the same sequence but with a single transmit/receive head coil. Pulse $\mathrm{FA_{sat}} = 500°$, $\mathrm{ENR} = 12.5°\,\mathrm{ms}^{-1}$

Peak location for uniform MTR histograms of the brain (PLUMB) plots were produced (see Fig. 2) as a simple way of visualising the change in peak location in single-slice (normalised) histograms, as a function of the slice position along the z-axis of the coil. The slices were ordered from inferior to superior. Because there is white matter in many of these slices, they give a simple, qualitative visualisation of how the peak MTR value is affected by B_1 changes along the superior–inferior (z- or caudal–rostral) axis of the subject [38]. The implementation was simply carried in a spreadsheet software package (Excel; *surface chart* option, Microsoft Corporation, Redmond, WA, USA). Contours were plotted, with choice over the level of each contour, and the colour between each contour.

Study 2: multi-coil study

Study 1 showed that the result from centre C (head-coil transmission) was very different from centres A and B (body-coil transmission) (see Fig. 1). Study 2 was designed to investigate whether, at a given centre, body-coil transmission could produce a narrower histogram.

At a fourth centre D, a single subject was imaged in two ways. First, the standard cylindrical transmit/receive birdcage coil, which is relatively uniform [39,40], was used. Second, a close-fitting phased-array receive-only *cap coil* was used with body-coil transmission. This cap coil is no longer available, but has been replaced by an eight-channel phased-array receive-only coil. PLUMB plots were again used to assist the comparison. The basic sequence was similar to that used in study 1, except that a more powerful MT pulse was used (Gaussian pulse [26], TR = 1,000 ms, $\mathrm{TR}' = 42$ ms, FA = 1,000°, hence $\mathrm{ENR} = 23.8°\,\mathrm{ms}^{-1}$). Forty-eight near-axial 3-mm slices were collected, with in-plane resolution of 0.94 mm. M_O and M_S images were registered before calculation of MTR maps.

Study 3: effect of MT pulse shape on histogram

Study 2 showed that body-coil transmission could indeed produce a narrower histogram (see Fig. 3). This supported the hypothesis that transmit nonuniformity is indeed a potentially major source of inter-centre variation. Head coils from different manufacturers could produce very different transmit-field distributions, depending on their particular design. This gave encouragement to undertake another multi-centre study, using two different manufacturers (centres B and D). The hypothesis was that by using body-coil transmission at both centres, identical histograms could be obtained. Although there would be some transmit nonuniformity arising from the head itself, this effect would not be manufacturer dependent.

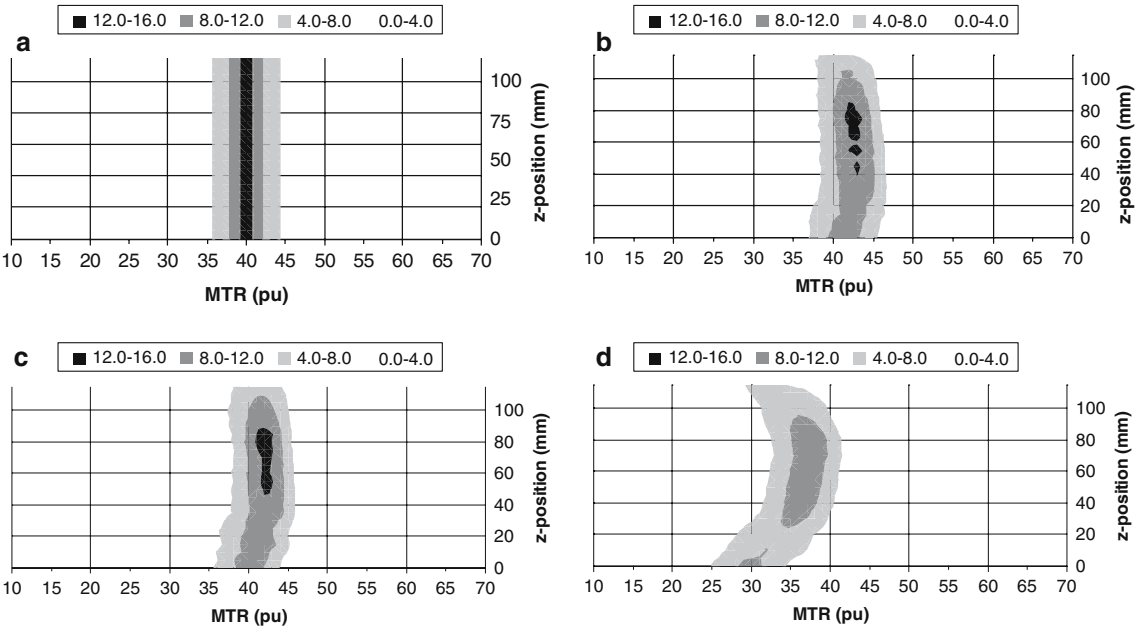

Fig. 2 **a** Test PLUMB plot for a peak located at 40 pu with amplitude 14.9. The legend shows the threshold histogram values for each of the four *shades of grey*. **b** PLUMB plot of group mean histogram from centre A (study 1; Fig. 1); *z*-position is from inferior to superior. **c** centre B **d** centre C

At first it was unclear exactly what pulse shape was being used at centre B. For a given MT pulse FA, how much difference would the shape make to the MTR histogram? Could a different pulse shape cause histogram broadening? A study of the effect of pulse shape was therefore made on a single subject at centre D (where different shapes could easily be programmed). The conventional Gaussian pulse, and also three- and five-lobed sinc pulses (duration 9.4 ms, bandwidths 617 and 408 Hz, respectively), were used, with both the birdcage T/R coil and an eight-channel receive-only (R/O) coil (body-coil transmission). Sequence parameters were as study 1 ($FA_{sat} = 500°$, $ENR = 12.5°ms^{-1}$).

Study 4: multi-centre study with body-coil transmission

Study 3 showed that the exact MT pulse shape had to be known, in order to match it another centre. A numerical description of the pulse at centre B was therefore obtained, and from this the analytic description of the pulse could be deduced, and a replicate programmed at centre D.

Five normal subjects were imaged at both centres (B and D), with different subjects at each centre, using body-coil transmission. At centre B four subjects were male, and the age range was 22–42 (median 31). At centre D there were also four male subjects, and the ages were very similar (range 26–55, median 29). An existing commercial three-dimensional spoilt-gradient-echo sequence at centre B was replicated at centre D. Parameters were: TR = TR′=106 ms, excitation (imaging) FA = 12°, MT pulse five-lobed sinc with Gaussian apodisation (standard deviation, SD = 0.5 × pulse width), $FA_{sat} = 620°$, offset 1,100 Hz, duration 15 ms. At centre B a quadrature receive coil was used, at centre D an eight-channel receive coil was used. Segmentation at centre B extracted the whole brain, followed by some manual removal of CSF; histograms had bins 1 pu wide, centrally labelled, and PL was estimated to within about 0.3 pu by manual interpolation. Segmentation at centre D was performed simply; the skull and other non-brain tissues, such as the orbits, were removed, but CSF was left in. The histograms bins were 0.1 pu wide.

Study 5: removal of residual inter-centre differences

A small inter-centre difference in PL of 1.2 pu was seen in study 4 (see Fig. 5). It was hypothesised that this might be caused by a small difference between centres in the pre-scan procedure for setting the imaging FA (this would then affect all pulses, including the MT pulse). A 2–4% error would be enough to explain the observed difference. It was further hypothesised that a small adjustment of the MT pulse FA would bring the histograms into complete alignment.

At centre D the dependence of PL on FA_{sat} was investigated in two normal subjects. From this it was estimated that increasing FA_{sat} from 620° to 652° would remove the small inter-centre difference. Five new subjects were scanned with the original value and this increased value (the other parameters were the same as for study 4). Three of these subjects were male, and ages were 25–39 (median 33).

The effect of segmentation was investigated by carrying out additional segmentation, at centre D, of all the image data-sets, using bin widths of both 1 and 0.1 pu. In addition, segmentation and histogram generation for individual tissue types [grey matter (GM) and white matter (WM)] was carried out, using a 0.1 pu bin width.

The design of the five studies are summarised in Table 2.

Table 2 Summary of studies

Study	Centre	Transmission coil	Manufacturer	Pulse (shape, FA_{sat}, TR′)	Figures
1. Multi-centre, initial	A	Body	1	Gauss, 500, 40	1,2
	B	Body	1		
	C	Tapering head	2		
2. Multi-coil	D	Body and birdcage head	3	Gauss, 1,000, 42	3
3. Effect of pulse shape	D	Body and birdcage head	3	Various, 500, 40	4
4. Multi-centre, body coil only	B	Body	1	Sinc5, 620, 106	5
	D	Body	3	Sinc5, 620, 106	
5a. Small variation in FA_{sat}	D	Body	3	Sinc5, 600–660, 106	6
5b. Adjust FA_{sat} to align centres	B	Body	1	Sinc5, 620, 106	7
	D	Body	3	Sinc5, 652, 106	

Results

Study 1: multi-centre study

Histograms from the three centres showed clear differences (Fig. 1, Table 3). Segmentation volumes agreed well (range of 2% in mean values). The group mean histograms from centres A and B (same manufacturer) were very similar (see Table 3), showing that excellent inter-centre agreement can be reached if the relevant factors are controlled (although a small but significant difference was found, see below).

After matching, the group mean histogram peak location and height from centres A and B were very close (Table 3), although the matching process had taken place over most of the histogram (including parts distant from the peak). However centre C, from a different manufacturer, had very different histograms; the peak was located lower and was broader. The matching process was unable to remove these remaining differences (Fig. 1).

Transforming individual histograms from centre A to centre B, using the LOO group matching procedure, gave remarkably similar transformations for each training set of five subjects. The scaling factor b (Eq. 3) varied from 1.012 to 1.015; root-mean-square residuals were small (range 0.08–0.10 %vol pu^{-1}). The changes to the six individual histograms were also remarkably consistent [PL change: mean −0.58 pu (SD = 0.10); PH change: mean 0.15%vol pu^{-1} (SD = 0.02)]. Before transformation, the PL of the A group (the six individuals scanned at centre A) was significantly higher than that of the B group (0.53 pu; one-tailed t test $p < 0.03$); after transformation the A and B groups were indistinguishable. Group differences in peak heights were not significant, either before or after transformation. The SD of the PL in the A and B groups combined (12 measurements) reduced from 0.49 pu before transformation to 0.40 pu after transformation, reflecting residual variations from between-subject and within-subject (including rescan) effects. The SD of the PH measurements was unaltered by transformation (0.69, 0.67%vol pu^{-1})

Table 3 Matching group mean histograms to target centre B(*)

	A	B(*)	C
Raw peak height (%vol pu^{-1})	11.20	11.58	8.73
Raw peak location (pu)	43.25	42.65	37.35
Full-width at half-maximum (pu)	6.3	6.1	8.6
Matched peak height (%vol pu^{-1})	11.35	–	7.66
Matched peak location (pu)	42.65	–	42.35
Root-mean-square residual (%vol pu^{-1})	0.088	–	1.42
Scaling factor b	1.013	–	0.88

After matching, all centres have peak location very close to that of centre B (42.6 pu); however only centre A (using the same manufacturer) has a similar peak height (11.6%vol pu^{-1}); in this case only a small amount of object scaling ($b = 1.013$) would explain the difference

The PLUMB plots were found to be convenient to use and easy to interpret, once suitable values for the contour levels and colours differences between the contours had been found.

Study 2: multi-coil study

An improvement was seen (see Fig. 3a) by changing from the birdcage to the receive-only cap coil; the peak was located higher, and was narrower. The PLUMB plot also looked straighter. Thus changing to body-coil excitation had removed some RF nonuniformity.

The peak location using body-coil transmission at centre D was much higher for this sequence (almost 62 pu; see Fig. 3a) than for the sequence used in study 1 (43 pu; see Fig. 1). This is consistent with the doubling of the ENR value (from 12.5 to 23.8° m s^{-1}). Peak height with this sequence was lower (possibly because of increased dispersion at the higher saturation power).

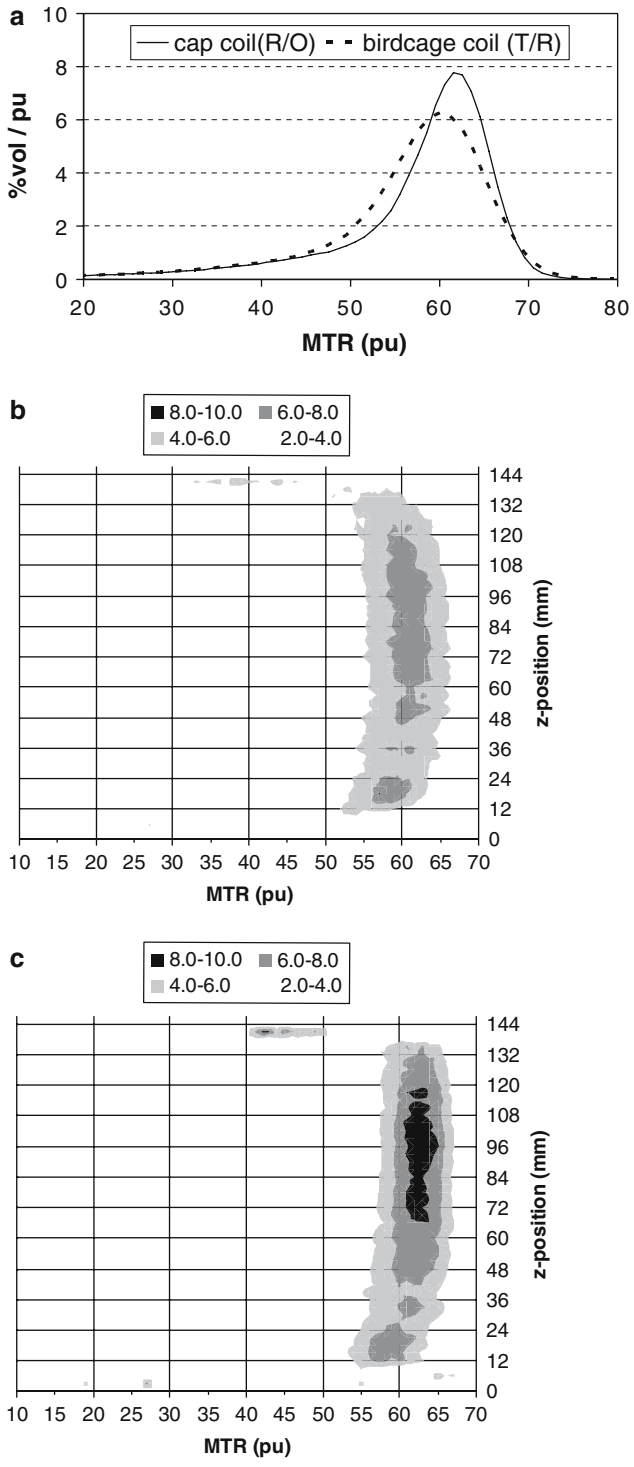

Fig. 3 Multi-coil study (study 2): transmit/receive (T/R) birdcage coil and receive-only (R/O) cap coil with body-coil transmit. **a** histograms: note that the R/O coil gives a higher (and therefore narrower) histogram. Pulse $FA_{sat} = 1,000°$, ENR = 23.8° ms^{-1}. **b** PLUMB plot for T/R birdcage coil; *z*-position is from inferior to superior. (NB the *grey scale* is different from that of Fig. 2, see legend.) **c** PLUMB plot for R/O cap coil

Study 3: effect of MT pulse shape on histogram

A progressive increase in MT effect was seen passing from the Gaussian shape, through the three-lobed to the five-lobed sinc (Fig. 4). Although these have the same FA, the power increases as side lobes are added. For each pulse shape, the eight-channel coil is seen to give a narrower histogram (with greater PH). The five-lobe sinc was so powerful that with body-coil transmission it exceeded SAR limits, and FA_{sat} had to be reduced slightly (to 450°). The PH is seen to increase with power, then decrease, possibly related to how the MTR values from the different brain tissues are dispersed with increasing power.

Study 4: multi-centre study with body-coil transmission

Group histograms were closer than had been achieved previously (Fig. 5a). PL showed a small inter-centre difference of 1.2 pu (Fig. 5b: centre B: mean = 35.96, SD = 0.3; centre D: mean = 34.74, SD = 0.7; two-tailed *t* test $p = 0.007$). Including age and gender in a generalised linear model did not remove this, so it was concluded to be a genuine centre effect, not one caused by the individual subjects. PH values were indistinguishable between centres B and D (Fig. 5c: two-tailed *t* test $p = 0.3$).

Study 5: removal of residual inter-centre differences

Both subjects had a similar dependence of PL on FA_{sat} (see Fig. 6). The mean slope was 0.38 pu deg^{-1}.

Using the increased value of $FA_{sat} = 652°$ at centre D and carrying out all segmentation at centre D with 0.1 pu bin widths gave group histograms that were very similar to those of centre B (Fig. 7a). PL values were indistinguishable (Fig. 7b: two-tailed *t* test $p = 0.5$). PH values were also indistinguishable (Fig. 7c: two-tailed *t* test $p = 0.6$; pooled mean 9.5%vol pu^{-1}).

Carrying out segmentation of centre B data at centre D instead of at B, (whilst keeping 1 pu bin widths) reduced the mean PH by about 25% (2.4%vol pu^{-1}; paired two-tailed *t* test, $p < 0.0001$; Fig. 8), which is consistent with the D segmentation including more CSF. Adjusting the segmentation at centre B produced alterations in PH, with a range of about 20%. Reducing the bin width from 1 to 0.1 pu increased the mean PH by about 15% (1.6%vol pu^{-1}; $p < 0.0003$), which is consistent with the peak structure smoothing expected when using 1 pu bin widths. Noise in small bins may also contribute to greater peak heights, depending on how much smoothing has been used. PL values were not affected by altering the segmentation or bin width. Histogram parameters for GM and WM were not significantly different between the two centres ($p > 0.4$). Pooled values (10 subjects from the two centres) were [mean (SD)]: GM PL

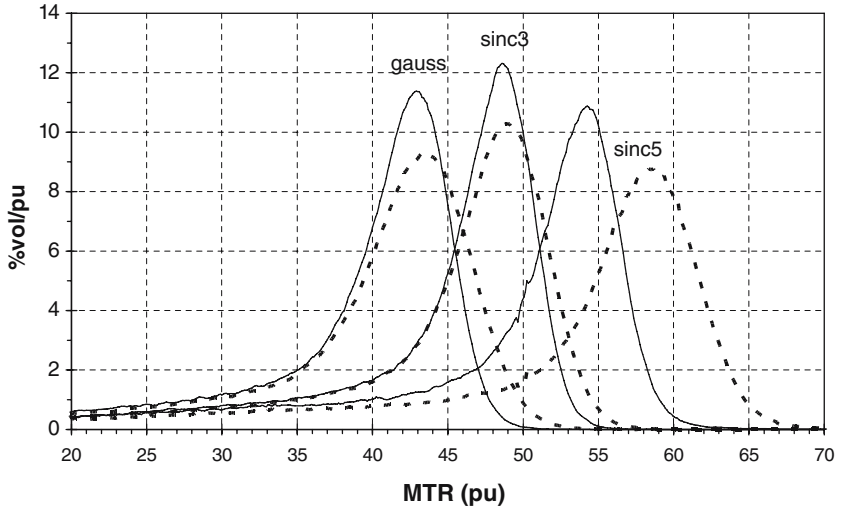

Fig. 4 Study 3 (multiple pulse shapes). Histograms from Gaussian, three-lobed sinc and five-lobed sinc are shown. Body-coil transmission (*solid lines*) produces histograms with greater PH that are narrower than those from the birdcage T/R coil (*dotted lines*). All pulses had $FA_{sat} = 500°$, $TR' = 40$ ms, ENR = 12.5° ms^{-1}, except that for the five-lobed sinc with body-coil excitation FA_{sat} had to be reduced to 450° because of SAR limitation

34.2 pu (0.6), PH 13.3%vol pu^{-1} (1.0); WM PL 37.3 pu (0.6), PH 18.8%vol pu^{-1} (1.5).

Discussion

Substantial evidence for the importance of transmit-coil nonuniformity in broadening histograms has been given (Figs. 3, 4). The poor performance in study 1 of centre C (Fig. 1) was almost certainly caused by the head coil being nonuniform. Although study 2 cannot be considered conclusive (since it was carried out on only one subject, Fig. 3), it does support our original hypothesis on body-coil transmission, and guided the way to the final outcome (Fig. 7). Study 3 (Fig. 4) suggests that altering the pulse shape alone cannot produce such dramatic histogram broadening. Studies 3 and 5 (Figs. 5, 7) suggest that, by using body-coil transmission, excellent inter-centre agreement can be reached. Gaussian pulses produce less MTR, and less power, than their sinc siblings with the same FA, although which of these produces more MTR for a given power is still not known (Fig. 4). PLUMB plots (Fig. 2) are a convenient way of visualising and comparing RF nonuniformity. A complete list of other potential sources of inter-centre difference has been given (Table 1). Segmentation and bin width are important factors if PH values are to be comparable (Fig. 8).

These data suggest that any serious multi-centre studies using MTR histograms have to use body-coil transmission (in addition to exactly the same MT pulse shape, MT pulse sequence parameters and segmentation procedure). Fortunately, with the advent of close-fitting multi-array head coils, which are usually receive-only, the major MRI manufacturers are now offering body-coil transmission as a standard feature. Body-coil excitation (transmission) may sometimes have a higher SAR (power deposition) than using a single head coil for excitation; however this may not be a serious problem, since the SAR increase may be minimal, and also maximal tissue contrast may be obtained (at least at 1.5 T) at sub-maximal SAR [41]. Thus any future multi-centre studies should use body-coil transmission as an essential prerequisite. There was some evidence from repeated imaging of significant between-subject variation (up to 1 pu in PL). Further attention to the imaging procedure might reduce this, and hence possibly also the measured normal within-group variation, thus increasing the sensitivity of studies to biological change. Segmentation is relatively easy to carry out at a single centre, since images can be transferred in a standard format (e.g. DICOM or Analyze).

A larger multi-centre study of normal controls would be desirable before embarking on a clinical trial, and this pilot shows how it should be set up. The study would use imagers only in body-coil transmission mode, and at first just locally recruited controls. After establishing good within-centre reproducibility for individuals, and good between-centre group agreement, a small number of controls could travel between centres. Any residual inter-centre differences could be taken into account in the statistical analysis.

Even with body-coil transmission, there will be residual B_1 nonuniformity, arising from two sources. Firstly, the body coil itself, although larger than a head coil,

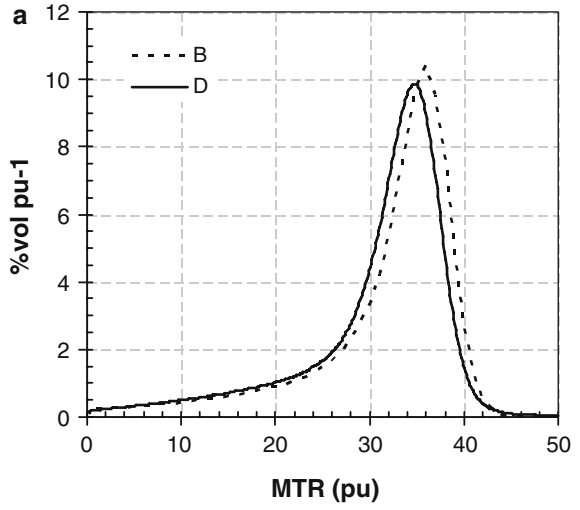

Fig. 5 Multi-centre study using body-coil excitation (study 4). Centres B and D both used five-lobed sinc pulses with $FA_{sat} = 620°$, $TR' = 104$ ms, ENR = 6.0° ms^{-1}. **a** Group histograms are very similar; **b** there is a small but significant residual difference in PL values (*circles*); **c** PH is indistinguishable between centres (*circles*). For later comparison, some study 5 data are also shown (*triangles* in parts **b** and **c**, both 620° from centre D)

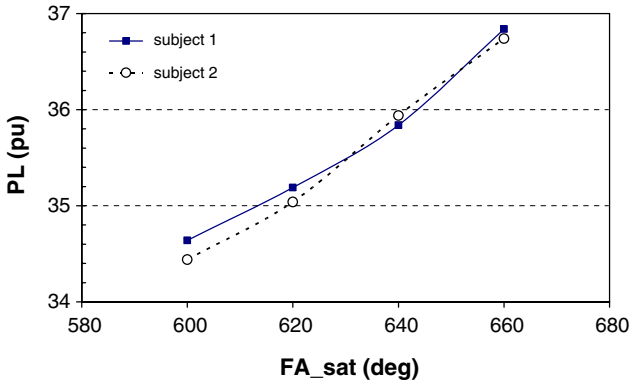

Fig. 6 Dependence of PL on FA_{sat}, in two control subjects (study 5)

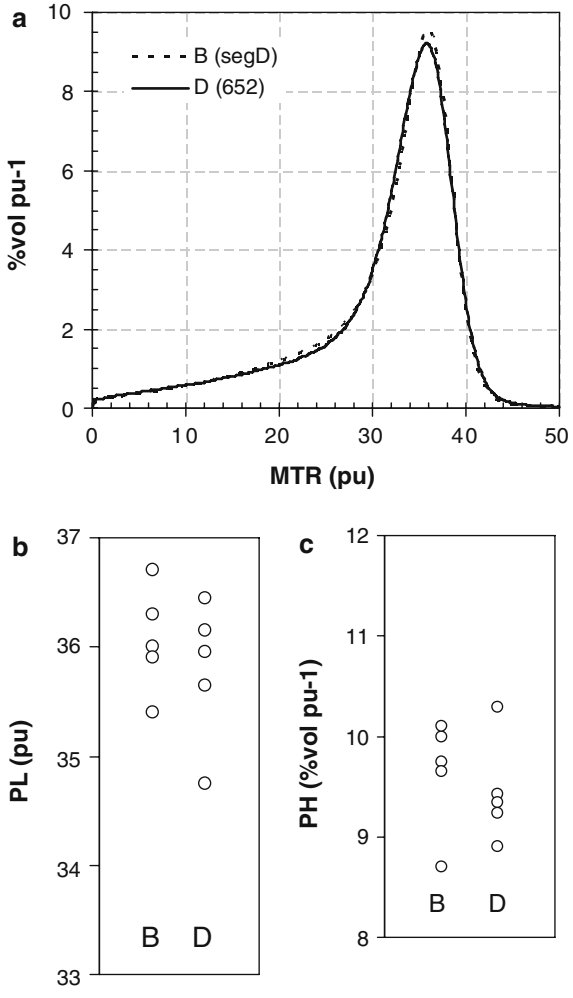

Fig. 7 Final multi-centre study using body-coil excitation, and all segmentation carried out at centre D (study 5). Centre B used $FA_{sat} = 620°$ (as in study 3, Fig. 5) whilst centre D used an increased $FA_{sat} = 652°$. $TR' = 104$ ms. **a** group histograms are almost indistinguishable; **b** and **c** peak locations and heights show no inter-centre difference

will still produce a transmit field that is slightly nonuniform; this will depend on the particular design and hence manufacturer. Secondly, RF nonuniformity will arise from the head itself (even in a perfectly uniform transmit field). Dielectric resonance (RF standing waves) increase B_1 near the centre of the head [42], whilst the electrical conductivity decreases it (through the skin effect). At 3 T and higher these effects become more pronounced [43]. Fortunately this second, intrinsic, source of RF nonuniformity is subject dependent, but not imager dependent, and thus will not contribute to within-subject or between-imager variation.

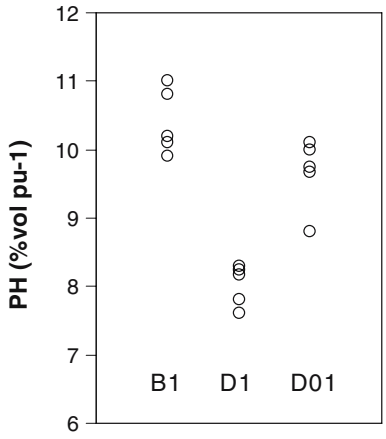

Fig. 8 Effect of segmentation and bin width on peak height. Five subjects from centre B were segmented with 1 pu bin width at B (B1), then at centre D (D1), then finally at D with 0.1 pu bin width (D01)

B_1 mapping has been used to reduce the effects of B_1 errors and nonuniformity on MTR values [24, 25]. The effect is reduced, and in one study [24] the between-centre difference in mean MTR values was completely eliminated (for three centres using two different manufacturers). However the correction does rely on all tissue types (e.g. grey and white matter) being treated in the same way, is therefore only an approximation, and is probably not accurate enough to remove between-centre differences in all histogram features. Other histogram features such as peak height and the area under one tail are often better indicators than mean MTR of heterogeneous disease [44]. These latter parameters have the benefit of being approximately independent of peak location, and thus of small B_1 errors arising from the auto-pre-scan procedure. These parameters, which essentially indicate heterogeneity within the volume of interest, are thus very sensitive to RF nonuniformity, and are likely to benefit enormously from body-coil transmission (see Figs. 2b, c, 3a).

Histogram matching is clearly too simplistic an approach to dealing with between-imager effects (Fig. 1). However it may be appropriate to correct the small between-centre effects for the same imager manufacturer, although these small effects may also be taken into account by suitable statistical analysis.

The PLUMB plot (Fig. 2) is a simple, easily implemented, way of visualising instrumental uniformity along the superior–inferior axis, although it does include some genuine biological changes along that axis of the brain (e.g. varying grey matter/white matter ratios). It does not evaluate within-slice nonuniformity (in the transverse directions). The peak height in each slice is indicative of the spread of MTR values (since the histogram is normalised to a fixed area).

Although many histogram studies have been published using the rather course resolution (bin width) of 1 pu, the data could possibly be retrospectively improved to give a resolution approaching the more desirable 0.1 pu, as follows. The data can be interpolated [21] from the neighbouring four points, to 0.1 pu resolution, using Everett's formula for cubic interpolation [45]. Alternatively the region of the peak can be fitted to a parabola or cubic expression.

Histograms of other parameters (e.g. T_1, diffusion, and quantitative MT parameters such as the bound-water fraction) can also be generated [3], and much of the conceptual analysis presented here is applicable to these other parameters. Mapping of reliable quantitative MT parameters [46–49], based on a binary spin-bath model, is sensitive to the factors that we have identified as being important for MTR. In addition it needs control of the location of the data points (in the space of MT pulse amplitude and offset frequency), and requires that the model being fitted is specified. Note that for quantitative MT parameters, B_1 errors can be accounted for in the model, provided they are known (which is not the case for MTR). Histograms of individual tissue types (normal-appearing grey and white matter) have also benefited from the approach we have described, (although segmentation might be best carried out using registered structural T_1-weighted images). Although the PL values (34.2 and 37.3 pu, respectively) did not differ much from that of the whole brain (35.9 pu, Fig. 7b), the PH values (13.3 and 18.8%vol pu^{-1}) were considerably higher than for whole brain (PH = 9.5, Fig. 7c), since they came from a much more homogeneous volume of tissue.

In conclusion, the six major categories of sources of variation in MTR histograms of the brain have been identified. Transmit nonuniformity is probably the major source for multi-centre studies. For future studies we recommend that body-coil transmission should be used, ideally with coils of the same design. Other factors such as MT pulse and sequence, segmentation and histogram generation can often be relatively easily controlled. To define peak height and location properly, MTR histograms should ideally have a 0.1 pu bin width, with a specified amount of smoothing. Imager stability is essential, although histogram parameters that are independent of peak location are probably robust to small transmitter changes.

Acknowledgments General Electric Medical Systems loaned the cap coil used in study 2. Gerard Davies and Frank Hoogenraad provided helpful discussion.

References

1. van Buchem MA, Tofts PS (2000) Magnetization transfer imaging. Neuroimaging Clin N Am 10:771–788
2. Tofts PS, Steens SCA, van Buchem MA (2003) MT: magnetization transfer (chapter 8). In: Tofts PS (ed.) Quantitative MRI of the brain: measuring changes caused by disease. Wiley, Chichester, pp. 257–298
3. Tofts PS, Davies GR, Dehmeshki J (2003) Histograms: measuring subtle diffuse disease (chapter 18). In: Tofts PS (ed.) Quantitative MRI of the brain: measuring changes caused by disease. Wiley, Chichester, pp. 581–610
4. van Buchem MA, Udupa JK, McGowan JC, Miki Y, Heyning FH, Boncoeur-Martel MP, Kolson DL, Polansky M, Grossman RI (1997) Global volumetric estimation of disease burden in multiple sclerosis based on magnetization transfer imaging. AJNR Am J Neuroradiol 18:1287–1290
5. Rovaris M, Bozzali M, Rodegher M, Tortorella C, Comi G, Filippi M (1999) Brain MRI correlates of magnetization transfer imaging metrics in patients with multiple sclerosis. J Neurol Sci 166:58–63
6. van Waesberghe JH, van Buchem MA, Filippi M, Castelijns JA, Rocca MA, van der BR, Polman CH, Barkhof F (1998) MR outcome parameters in multiple sclerosis: comparison of surface-based thresholding segmentation and magnetization transfer ratio histographic analysis in relation to disability (a preliminary note). AJNR Am J Neuroradiol 19:1857–1862
7. Filippi M, Iannucci G, Tortorella C, Minicucci L, Horsfield MA, Colombo B, Sormani MP, Comi G (1999) Comparison of MS clinical phenotypes using conventional and magnetization transfer MRI. Neurology 52:588–594
8. Davies GR, Ramio-Torrenta L, Hadjiprocopis A, Chard DT, Griffin CM, Rashid W, Barker GJ, Kapoor R, Thompson AJ, Miller DH (2004) Evidence for grey matter MTR abnormality in minimally disabled patients with early relapsing-remitting multiple sclerosis. J Neurol Neurosurg Psychiatr 75:998–1002
9. Bosma GP, Rood MJ, Huizinga TW, de Jong BA, Bollen EL, van Buchem MA (2000) Detection of cerebral involvement in patients with active neuropsychiatric systemic lupus erythematosus by the use of volumetric magnetization transfer imaging. Arthritis Rheum 43:2428–2436
10. Steens SC, Admiraal-Behloul F, Bosma GP, Steup-Beekman GM, Olofsen H, Le CS, Huizinga TW, van Buchem MA (2004) Selective gray matter damage in neuropsychiatric lupus. Arthritis Rheum 50:2877–2881
11. Patel UJ, Grossman RI, Phillips MD, Udupa JK, McGowan JC, Miki Y, Wei L, Polansky M, van Buchem MA, Kolson D (1999) Serial analysis of magnetization-transfer histograms and Expanded Disability Status Scale scores in patients with relapsing–remitting multiple sclerosis. AJNR Am J Neuroradiol 20:1946–1950
12. Rocca MA, Mastronardo G, Rodegher M, Comi G, Filippi M (1999) Long-term changes of magnetization transfer-derived measures from patients with relapsing–remitting and secondary progressive multiple sclerosis. AJNR Am J Neuroradiol 20:821–827
13. Filippi M, Inglese M, Rovaris M, Sormani MP, Horsfield P, Iannucci PG, Colombo B, Comi G (2000) Magnetization transfer imaging to monitor the evolution of MS: a 1-year follow-up study. Neurology 55:940–946
14. Rovaris M, Agosta F, Sormani MP, Inglese M, Martinelli V, Comi G, Filippi M (2003) Conventional and magnetization transfer MRI predictors of clinical multiple sclerosis evolution: a medium-term follow-up study. Brain 126:2323–2332
15. Davies GR, Altmann DR, Rashid W, Chard DT, Griffin CM, Barker GJ, Kapoor R, Thompson AJ, Miller DH (2005) Emergence of thalamic magnetization transfer ratio abnormality in early relapsing–remitting multiple sclerosis. Mult Scler 11:276–281
16. Davies GR, Altmann DR, Hadjiprocopis A, Rashid W, Chard DT, Griffin CM, Tofts PS, Barker GJ, Kapoor R, Thompson AJ, Miller DH (2005) Increasing normal-appearing grey and white matter magnetisation transfer ratio abnormality in early relapsing–remitting multiple sclerosis. J Neurol 252:1037–1044
17. Berry I, Barker GJ, Barkhof F, Campi A, Dousset V, Franconi JM, Gass A, Schreiber W, Miller DH, Tofts PS (1999) A multicenter measurement of magnetization transfer ratio in normal white matter. J Magn Reson Imaging 9:441–446
18. Barker GJ, Tofts PS, Gass A (1996) An interleaved sequence for accurate and reproducible clinical measurement of magnetization transfer ratio. Magn Reson Imaging 14:403–411
19. Sormani MP, Iannucci G, Rocca MA, Mastronardo G, Cercignani M, Minicucci L, Filippi M (2000) Reproducibility of magnetization transfer ratio histogram-derived measures of the brain in healthy volunteers. AJNR Am J Neuroradiol 21:133–136
20. Horsfield MA, Barker GJ, Barkhof F, Miller DH, Thompson AJ, Filippi M (2003) Guidelines for using quantitative magnetization transfer magnetic resonance imaging for monitoring treatment of multiple sclerosis. J Magn Reson Imaging 17:389–397
21. Tofts PS, Steens SCA, Dehmeshki J, Hofman P, van Waesberghe JH, van Buchem MA (2001) Matching MTR histograms for Multi-Centre Studies. In: Proceedings of the International Society for magnetic resonance in medicine, 9th annual meeting, Glasgow, pp. 1380
22. Tofts PS, Yeung R, Barker GJ (2002) Improvement in MTR histogram multi-centre performance using a receive-only head coil: the PLUMB plot. In: Proceedings of the International Society for magnetic resonance in medicine, 10th annual meeting, Honolulu, pp. 2283
23. Tofts PS, Steens SC, Cercignani M, Tozer DJ, Teeuwisse WM, van Osch MJ, Admiraal-Behloul F, Barker GJ, van Buchem MA (2006) Intercentre differences in multicentre brain MTR histogram studies can almost be eliminated by using body coil transmission. In: Proceedings of the International Society for magnetic resonance in medicine, 14th annual meeting, Seattle
24. Ropele S, Filippi M, Valsasina P, Korteweg T, Barkhof F, Tofts PS, Samson R, Miller DH, Fazekas F (2004) Assessment and correction of B(1)-induced errors in magnetization transfer ratio measurements. Magn Reson Med 53:134–140
25. Samson RS, Wheeler-Kingshott CA, Symms MR, Tozer DJ, Tofts PS (2006) A simple correction for B1 field errors in magnetization transfer ratio measurements. Magn Reson Imaging 24(3):255–263

26. Barker GJ, Schreiber WG, Gass A, Ranjeva JP, Campi A, van Waesberghe JH, Franconi JM, Watt HC, Tofts PS (2005) A standardised method for measuring magnetisation transfer ratio on MR imagers from different manufacturers – the EuroMT sequence. Magn Reson Mater Phy 18:76–80
27. Pekar J, Jezzard P, Roberts DA, Leigh Jr JS, Frank JA, McLaughlin AC (1996) Perfusion imaging with compensation for asymmetric magnetization transfer effects. Magn Reson Med 35:70–79
28. van Buchem MA, McGowan JC, Kolson DL, Polansky M, Grossman RI (1996) Quantitative volumetric magnetization transfer analysis in multiple sclerosis: estimation of macroscopic and microscopic disease burden. Magn Reson Med 36:632–636
29. Cercignani M, Symms MR, Schmierer K, Boulby PA, Tozer DJ, Ron M, Tofts PS, Barker GJ (2005) Three-dimensional quantitative magnetisation transfer imaging of the human brain. Neuroimage 27:436–441
30. Stevenson VL, Parker GJ, Barker GJ, Birnie K, Tofts PS, Miller DH, Thompson AJ (2000) Variations in T1 and T2 relaxation times of normal appearing white matter and lesions in multiple sclerosis. J Neurol Sci 178:81–87
31. Tofts PS (2003) PD: proton density of tissue water (chapter 4). In: Tofts PS (ed.) Quantitative MRI of the brain: measuring change caused by disease. Wiley, Chichester, pp. 85–109
32. Jost G, Hahnel S, Heiland S, Stippich C, Bellemann ME, Sartor K (2002) An automated method for volumetric quantification of magnetization transfer of the brain. Magn Reson Imaging 20:593–597
33. Tozer DJ, Tofts PS (2003) Removing spikes caused by quantization noise from high-resolution histograms. Magn Reson Med 50:649–653
34. Fernando KT, Tozer DJ, Miszkiel KA, Gordon RM, Swanton JK, Dalton CM, Barker GJ, Plant GT, Thompson AJ, Miller DH (2005) Magnetization transfer histograms in clinically isolated syndromes suggestive of multiple sclerosis. Brain 128:2911–2925
35. Hofman PA, Kemerink GJ, Jolles J, Wilmink JT (1999) Quantitative analysis of magnetization transfer images of the brain: effect of closed head injury, age and sex on white matter. Magn Reson Med 42:803–806
36. Dehmeshki J, Barker GJ, Tofts PS (2002) Classification of disease subgroup and correlation with disease severity using magnetic resonance imaging whole-brain histograms: application to magnetization transfer ratios and multiple sclerosis. IEEE Trans Med Imaging 21:320–331
37. Udupa JK, Odhner D, Samarasekera S, Goncalves RJ, Venugopal KP, Furule SS (1994) 3DVIEWUNIX: an open, transportable, multidimensional, multimodality, multiparametric imaging software system. SPIE Proc 2164:58–73
38. Silver NC, Barker GJ, Gass A, Schreiber W, Miller DH, Tofts PS (1997) Magnetisation transfer ratio measurements of the brain depend on the region of interest position within the head coil. In: Proceedings of the International Society of magnetic resonance in medicine, 5th Annual meeting, Vancouver, pp. 662
39. Barker GJ, Simmons A, Arridge SR, Tofts PS (1998) A simple method for investigating the effects of non-uniformity of radiofrequency transmission and radiofrequency reception in MRI. Br J Radiol 71:59–67
40. Whittall KP, MacKay AL, Graeb DA, Nugent RA, Li DK, Paty DW (1997) In vivo measurement of T2 distributions and water contents in normal human brain. Magn Reson Med 37:34–43
41. Graham SJ, Henkelman RM (1999) Pulsed magnetization transfer imaging: evaluation of technique. Radiology 212:903–910
42. Tofts PS (1994) Standing waves in uniform water phantoms. J Magn Reson series B 104:143–147
43. Collins CM, Smith MB (2001) Signal-to-noise ratio and absorbed power as functions of main magnetic field strength, and definition of "90 degrees " RF pulse for the head in the birdcage coil. Magn Reson Med 45:684–691
44. Tofts PS, Benton CE, Tozer DJ, Jäger HR, Waldman AD, Rees JH (2005) Quantitative histogram analysis of Gd enhancement in low grade gliomas may predict malignant transformation. In: Proceedings of the International Society for magnetic resonance in medicine, 13th annual meeting, Miami, p. 754
45. Scheid F (1968) Schaum's outline of theory and problems of numerical analysis. McGraw–Hill, New York
46. Ramani A, Dalton C, Miller DH, Tofts PS, Barker GJ (2002) Precise estimate of fundamental in-vivo MT parameters in human brain in clinically feasible times. Magn Reson Imaging 20:721–731
47. Sled JG, Pike GB (2001) Quantitative imaging of magnetization transfer exchange and relaxation properties in vivo using MRI. Magn Reson Med 46:923–931
48. Yarnykh VL (2002) Pulsed Z-spectroscopic imaging of cross-relaxation parameters in tissues for human MRI: theory and clinical applications. Magn Reson Med 47:929–939
49. Tofts PS, Cercignani M, Tozer DJ, Symms MR, Davies GR, Ramani A, Barker GJ (2005) Errata: Tozer et al. Quantitative magnetization transfer mapping of bound protons in multiple sclerosis, Magn Reson Med 2003;50:83–91. Magn Reson Med 53:492–493